

Report Title: **Novel Nanocrystalline Intermetallic Coatings for Metal Alloys  
in Coal-fired Environments**

Type of Report: Final

Report Period: September 2005 / September 2009

Principle Investigator: Professor Z. Zak Fang  
Tel. (801)581-8128  
Email: [zak.fang@utah.edu](mailto:zak.fang@utah.edu)  
Co-PI: Prof. H. Y. Sohn,  
Tel. (801)581-5491  
Email: [h.y.sohn@utah.edu](mailto:h.y.sohn@utah.edu)

Date Report Was Issued: January 8, 2010

DOE Award Number: DE-FG26-05NT42529

Submitting Organization: University of Utah  
Salt Lake City, UT 84102

**Acknowledgment:**

This report is based upon work supported by the U. S. Department of Energy under Award No. DE-FG26-05NT42529

**Disclaimer:**

This report was prepared as an account of work sponsored by an agency of the United States Government. Neither the United States Government nor any agency thereof, nor any of their employees, makes any warranty, express or implied, or assumes any legal liability or responsibility for the accuracy, completeness, or usefulness of any information, apparatus, product, or process disclosed, or represents that its use would not infringe privately owned rights. Reference herein to any specific commercial product, process, or service by trade name, trademark, manufacturer, or otherwise does not necessarily constitute or imply its endorsement, recommendation, or favoring by the United States Government or any agency thereof. The views and opinions of authors expressed herein do not necessarily state or reflect those of the United States Government or any agency thereof.

**Proprietary Data Notice:**

None.

## Table of Contents

Abstract .....	4
1 Introduction .....	5
2 Experimental .....	8
2.1 PTA coating process of iron aluminide .....	8
2.2 PTA coating process of nickel aluminide .....	9
2.3 Characterization of obtained aluminide coatings .....	10
2.3.1 Evaluating the bonding strength between coatings and substrates .....	10
2.3.2 Evaluating the corrosion resistance of the coatings in the atmosphere simulating the steam-side corrosion environment .....	11
2.3.3 Evaluating the corrosion resistance of the coatings under the conditions simulating the fire-side corrosion environment .....	12
2.3.4 Preparing Fe <sub>3</sub> Al coated stainless steel pipe for field-test in power plant .	14
3 Results and Discussion .....	16
3.1 Iron aluminide coatings .....	16
3.1.1 Iron aluminide coatings with iron aluminide powder as feed material ....	16
3.1.2 Iron aluminide coatings with blend of elemental iron and aluminum powders as the feed material .....	18
3.1.3 Iron aluminide coatings with aluminum powder as the feed material ....	19
3.1.4 Corrosion resistance of the coatings .....	23
3.1.5 Discussion .....	26
3.2 Nickel aluminide coatings .....	28
3.3 Field-testing Fe <sub>3</sub> Al coating in power plant .....	32

4	Conclusions .....	33
	Accomplishments .....	35
	References .....	36

## **Abstract**

Intermetallic coatings (iron aluminide and nickel aluminide) were prepared by a novel reaction process. In the process, the aluminide coating is formed by an in-situ reaction between the aluminum powder fed through a plasma transferred arc (PTA) torch and the metal substrate (steel or Ni-base alloy). Subjected to the high temperature within an argon plasma zone, aluminum powder and the surface of the substrate melt and react to form the aluminide coatings. The prepared coatings were found to be aluminide phases that are porosity-free and metallurgically bonded to the substrate. The coatings also exhibit excellent high-temperature corrosion resistance under the conditions which simulate the steam-side and fire-side environments in coal-fired boilers. It is expected that the principle demonstrated in this process can be applied to the preparation of other intermetallic and alloy coatings.

## 1. Introduction

In many industrial high-temperature applications including those in coal-fired environments, both high-temperature strength and high-temperature corrosion-resistance are required. However, it is usually very difficult to develop steels and alloys that can satisfy both these requirements [1]. Therefore, a high-temperature corrosion-resistant coating on a base alloy that has superior high temperature strength is both technically and economically attractive for these applications.

The aluminide intermetallics, such as iron aluminide ( $\text{Fe}_3\text{Al}$ ) and nickel aluminide ( $\text{Ni}_3\text{Al}$ ) are among the best candidates as a high-temperature corrosion-resistant coating materials. In general, these intermetallics have superior resistance to oxidation [2-5] and sulfidation [6-9] at high temperatures. It also exhibits other generally desired attributes such as low density, good wear resistance, and low cost [10-13]. However, the industrial applications of aluminide intermetallics as bulk components have been limited because of its low ductility, which poses considerable technical challenges for fabricating bulk components [10-13]. Using aluminide intermetallics as coatings in high temperature applications is a logical approach to take advantages of its superior high-temperature corrosion-resistance while avoiding the challenges of fabricating bulk components. Aluminide intermetallics coating is especially attractive for the power generation industry which has been making great efforts to increase the efficiency of coal-fired boilers by increasing the operating temperature and steam pressure. These conditions require better corrosion resistance [1]. Other possible industrial applications of aluminide intermetallics coatings include reactors for coal gasification, gas turbine, advanced gas-cooled nuclear reactor and so on, when high-temperature corrosion-resistance is critical.

Aluminide intermetallics coatings have been explored with various coating processes,

among which two categories of processes are notable: **a)** reaction coating processes including conventional chemical vapor deposition (CVD) processes [14], fluidized bed reactor CVD (FBR-CVD) [15-16] process, and pack cementation process [17-20], for producing thin coatings with thicknesses typically less than 20  $\mu\text{m}$ ; and **b)** thermal spray processes for making thick coatings with thicknesses from 0.5 to  $>3$  mm [21-26]. For many structural applications, including coal-fired power generation systems, thick coatings are often necessary due to the severe environments of high-temperature corrosion and erosion and the required long service lifetime. Therefore, thermal spray processes of several variations are the only viable options for making thick aluminide coatings.

Many thermal spray coating techniques, such as arc spray [21], low pressure plasma spray [22], air plasma spray [23] and high velocity oxyfuel (HVOF) spray [24-28], have been explored for depositing thick aluminide coatings on various steel substrates, with aluminide powder as the feeding materials. Among the above processes, the HVOF process is most attractive because the high velocity of sprayed and melted powders in this process produces coatings with higher density and better bonding to substrates than the coatings obtained with conventional thermal spray processes. However, even with HVOF processes, aluminide coatings with *full* density are still difficult to obtain. Porosity and oxide inclusions are always found in the HVOF aluminide coatings. Furthermore, the mechanical bonding between HVOF aluminide coatings and substrates is often unsatisfactory for demanding applications, and the oxidation-resistance of the coatings is found to be inferior to bulk aluminide intermetallics [28].

In this study, aluminide coatings were applied using a different coating technique – the plasma transferred arc (PTA) process. The unique advantage of the PTA process in comparison with other thermal spray processes is that the substrate is part of the power circuit so that the

substrate surface can be heated up to its melting temperature, which enables a metallurgical bonding between the coating and the substrate. Another important advantage of PTA process is that the coating layer is usually completely melted during the process so that porosities and oxide inclusions can be kept to minimum.

Based on the literature studies, there are only two reported studies to date in which PTA has been used to apply coatings of intermetallic compounds, NiTi [29] and NiAl [30]. There is no report on applying coatings of the targeted materials of present study, i.e., Fe<sub>3</sub>Al and Ni<sub>3</sub>Al.

As a straightforward concept, aluminide coatings can be applied on metal alloy substrates using PTA process by feeding pre-alloyed Fe<sub>3</sub>Al or Ni<sub>3</sub>Al powder, which is commercially available, as the raw material. Usually, the pre-alloyed aluminide powder is produced using gas atomization processes. It was thought possible, however, that the Fe<sub>3</sub>Al (or Ni<sub>3</sub>Al) coatings could be formed by feeding blends of elemental aluminum and iron (or nickel) powders, considering the strong tendency for iron (or nickel) and aluminum to react because of the large heat of reaction [31]. This would be more cost effective than using pre-alloyed Fe<sub>3</sub>Al (or Ni<sub>3</sub>Al) powder. Furthermore, aluminide coating can be expected to form, even if pure aluminum powder is fed, by an in-situ reaction between the fed Al and the Fe (or Ni) present in the steel (or Ni-base alloy) substrates. The reaction and the coating processes would be accomplished in one-step.

Therefore, the present project investigated the preparation method of Fe<sub>3</sub>Al and Ni<sub>3</sub>Al coatings by PTA process as well as the corrosion resistance performance of the prepared coatings. Considering the fact of the extensive applications of Fe<sub>3</sub>Al coatings on various grades of steel tubings in coal-fired environments, more efforts in the present study were put on Fe<sub>3</sub>Al coatings on steel substrates in comparison with Ni<sub>3</sub>Al on Ni-based alloy substrates. Field tests on the corrosion-resistant performance of the prepared Fe<sub>3</sub>Al coatings were also conducted in a

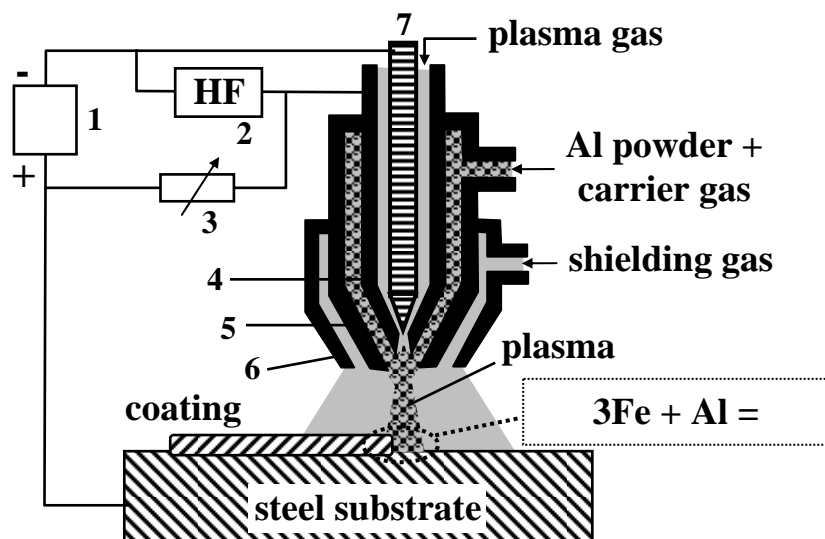


coal-fired power plant.

## 2. Experimental

### 2.1 PTA coating process of iron aluminide

Figure 1 schematically illustrates the PTA coating process. The PTA equipment used in this study for all coating tests is a Starweld Microstar 150 manufactured by Stellite Coatings. (Note: Starweld Microstar is a trade mark of Stellite Coatings). The distance between the plasma torch and the substrate was less than 12 mm to prevent the plasma from dying off. Three gas flows were used during the PTA process: the first gas flow was used to ignite and maintain the plasma between the torch and the substrate; the second gas flow was used as the carrier gas for feeding powder through a nozzle into the hot zone; and finally the third gas flow was used to provide a protective gas shield surrounding the hot zone to prevent oxidation of the coating as well as the substrate.



1. Power source
2. Oscillation unit
3. Ballast resistance
4. Plasma nozzle
5. Focusing nozzle
6. Shielding nozzle
7. Electrode

Fig.1 Schematic of the proposed coating process.

For the iron aluminide coatings, three series of coating tests were conducted in which a different feed material was used in each series. In Series A, iron aluminide powder was used as the feed material; in Series B, a blend of elemental aluminum and iron powders; while in Series C, pure aluminum powder. The iron aluminide powder used in Series A, was acquired from Ametek Specialty Metals, with the compositions of 15.4wt% Al, 5.8wt% Cr and Fe as the balance and the particle sizes of 44 to 149  $\mu\text{m}$ . For Series B, electrolytic iron powder (>99wt% Fe) of <149  $\mu\text{m}$  size was used. The aluminum powder (>99.8wt% Al) used in Series B and C was of 44-420  $\mu\text{m}$  size. The substrates were plain low-carbon steel coupons of 12.7 mm thickness, 38.1 mm width and 76.2 mm length.

During the coating process, the raw material powder from a feeder was carried by the carrier gas and fed through the plasma torch. As can be seen in the figure, the steel substrate was part of the power circuit and the plasma was generated between the torch and the substrate. Consequently, the temperature on the top surface of the substrate can be high enough to melt not only the fed powder, but also a thin surface layer of the substrate. Thus, as stated earlier, the melted feed powders are expected to react with the melted surface layer of the steel substrate to form the iron aluminide coatings.

## **2.2 PTA coating process of nickel aluminide**

For the nickel aluminide coatings, one series of coating tests were conducted in which only pure aluminum powder was used as the feed materials so that the nickel aluminide coatings were formed by the in-situ reaction of the fed aluminum and the Ni-base alloy substrate. The used Ni-based alloy substrate was Inconel 600 with the composition at% of Ni 73, Cr 17.3 and Fe 9.7.

## 2.3 Characterization of obtained aluminide coatings

After the coating process, the samples were air cooled to room temperature. The specimens were then sectioned and polished for metallographic examinations. Energy Dispersive X-ray analysis (EDAX) was used to measure the composition profiles across the coating layers. X-ray diffraction (XRD) analysis was used to identify the phases therein.

### 2.3.1 Evaluating the bonding strength between the coatings and the substrates

The testing and evaluations of the bonding strength between the coatings and the substrates is one of the most important tasks determining whether or not the proposed coating technology has any potential to be used in boiler applications. To evaluate the bonding strength, we conducted three-point bending tests as illustrated schematically in Figure 2. When the bonding strength equals or exceeds that of either the substrate or the coating material, the bending specimen will fracture along the transverse plane. When the bonding strength is inadequate, delamination will likely occur as shown in the figure.

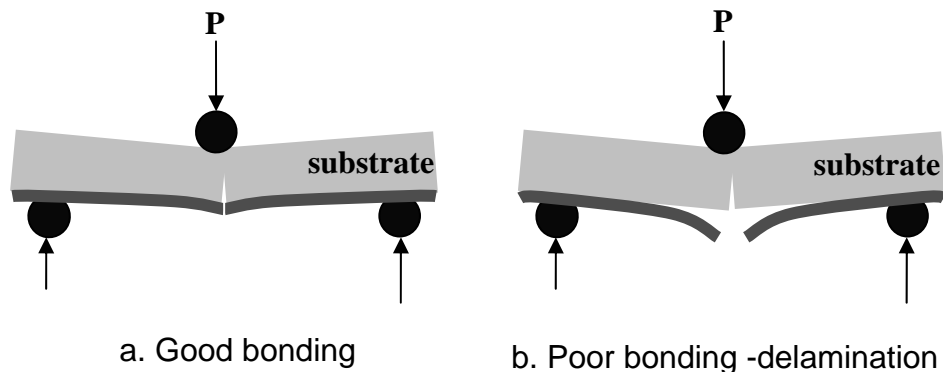


Fig. 2. A schematic illustration of bending tests for evaluation of the bonding strength of the coating to the substrate.

The samples for three-point bending tests were cut and then polished to the required dimensions (5 mm thick, 6.5 mm wide and 33 mm long). Among the total of 5 mm thickness, the

coating layer thickness was 1 mm and the substrate thickness was 4 mm.

### 2.3.2 Evaluating the corrosion resistance of the coatings in the atmosphere simulating the steam-side corrosion environment

To evaluate the steam-side corrosion resistance of the obtained coatings, corrosion tests in an atmosphere of the mixture of air and water vapor (with 10 vol% water vapor) were conducted at the temperature of 800°C. This condition is for accelerated oxidation simulating a worst scenario as the environment inside the boiler tube.

Figure 3 is the schematic of the experimental set-up of the corrosion tests.

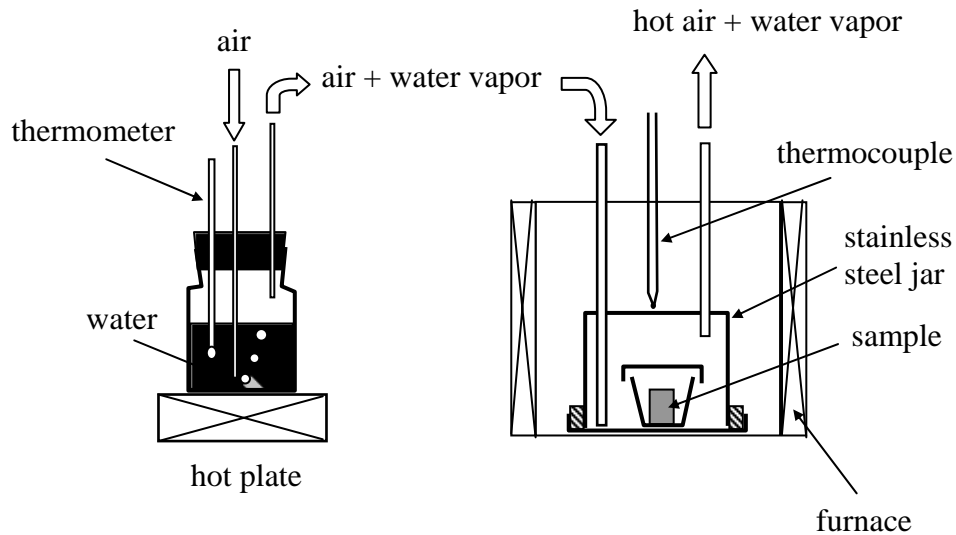


Fig. 3. Schematic of experimental set-up to evaluate the steam-side corrosion resistance

The samples for the corrosion tests were cut and then polished to the required dimensions (~10 mm wide and ~15mm long). After polishing, the coating layer thickness was ~2 mm and the substrate thickness was 16 mm. Stainless steel (304) samples were also tested in the same test runs in order to be compared with Fe<sub>3</sub>Al coating samples in terms of their corrosion resistance

performance.

The experimental procedure was as follows: Samples of  $\text{Fe}_3\text{Al}$  (coated on steel substrate) and stainless steel, each placed in a ceramic crucible with cap, were put inside a jar of stainless steel. Then the jar with all the samples was placed into a muffle furnace to be heated up according to a pre-designed 4-cycle profile with each cycle to be  $20^\circ\text{C}/\text{min}$  up to  $800^\circ\text{C}$ ,  $800^\circ\text{C}\times 20\text{h}$  and  $10^\circ\text{C}/\text{min}$  down to  $300^\circ\text{C}$ . The atmosphere of air + 10 vol% water vapor in the jar was maintained through continuously flowing the gas mixture of air + 10vol% water vapor into the jar. The gas mixture was produced by bubbling air in a distilled water bath at a pre-determined temperature ( $42^\circ\text{C}$  for obtaining the required 10vol% water vapor in the mixture). After the pre-determined cycles, the samples were removed from the jar to be cut, mounted and polished for microscopic observations.

### 2.3.3 Evaluating the corrosion resistance of the coatings under the conditions simulating the fire-side corrosion environment

To evaluate the fire-side corrosion resistance of the obtained coatings, corrosion tests were conducted under the conditions simulating a worst scenario as the environment outside the boiler tube.

Figure 4 is a schematic of the experimental set-up of the corrosion tests. The  $\text{Fe}_3\text{Al}$  samples for the corrosion tests were cut from the  $\text{Fe}_3\text{Al}$  layer coated on the common steel coupon and then polished to the required dimensions (~10 mm wide, ~15mm long and ~2 mm thick). Stainless steel (304) samples (~12 mm wide, ~15mm long and ~2.5 mm thick) were also tested in the same test runs in order to be compared with  $\text{Fe}_3\text{Al}$  samples in terms of their corrosion resistance performance.

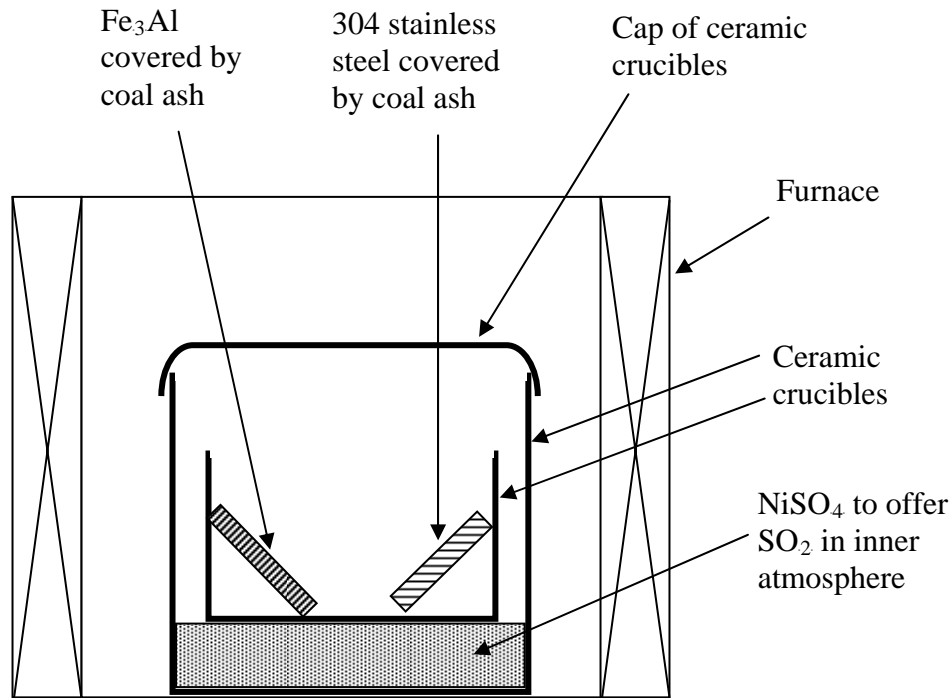


Fig. 4. Schematic of experimental set-up to evaluate the fire-side corrosion resistance

The fire-side environment was simulated with coal ash and flue gas. The synthetic coal ash fine powder was obtained by the following procedure: a) Sintering a mixture of chemical reagents with a desired composition (wt%): 5 Na<sub>2</sub>SO<sub>4</sub>, 5 K<sub>2</sub>SO<sub>4</sub>, 30 Al<sub>2</sub>O<sub>3</sub>, 30 SiO<sub>2</sub> and 30 Fe<sub>2</sub>O<sub>3</sub> at 800°C for 24 hours; b) Crashing and then wet-milling the sintered mixture in the media of heptane for 24 hours to obtain synthetic coal ash powder suspended in heptane. The surfaces of Fe<sub>3</sub>Al and stainless steel samples were cleaned with ethanol and then applied a layer of coal ash powder suspended in heptane with a brush.

The flue gas consisted of SO<sub>2</sub> and air. In this study, SO<sub>2</sub> in the atmosphere was supplied by placing sufficient amount of NiSO<sub>4</sub> powder surrounding the crucible inside which the Fe<sub>3</sub>Al and stainless steel samples were placed. According to the thermodynamic calculation based on decomposition reaction of NiSO<sub>4</sub> into NiO, SO<sub>2</sub> and O<sub>2</sub>, 5 vol% SO<sub>2</sub> would be maintained at

800°C in the air. Thus, during the corrosion tests of this study where the temperature was set to be 800°C, the flue gas was 5 vol% SO<sub>2</sub>, 20 vol% O<sub>2</sub> and 75 vol% N<sub>2</sub>.

#### 2.3.4 Preparing Fe<sub>3</sub>Al coated stainless steel pipes for field-test in power plant

Based on the superior corrosion resistance of Fe<sub>3</sub>Al coating observed from the preliminary corrosion tests simulating environments at both steam- and fire-side, field-tests were planned to be conducted in a power plant to evaluate the corrosion resistance performance of Fe<sub>3</sub>Al coating in realistic environments where this coating is desired to be used. Therefore, a series of coating experiments were conducted to prepare Fe<sub>3</sub>Al coated stainless steel pipes for scheduled field-tests in power plant.

Stainless steel pipes were actually half-circle pieces cut from whole pipes. These half-circle pieces are going to be mounted as shields for pipe in a boiler. The shield is expected to offer corrosion protection for the inner pipes in which water and steam flow. In comparison with the previous coating experiments on thick steel coupons, coating experiments on half-circle pieces required much more efforts to minimize the deformation of substrates during the coating process. Free standing half-circle pieces suffered significant distortion during the coating process, while a custom designed fixture during coating proved to be an effective approach for minimizing the distortion as shown in Figures 5 and 6. Microscopic observation also indicated that good metallurgical bonding formed between Fe<sub>3</sub>Al coating and stainless steel semi-pipe.



Figure 5. Overview of Fe<sub>3</sub>Al coated on half-circle-shaped 304 stainless steel



Figure 6. Cross-sectional view of Fe<sub>3</sub>Al coated on half-circle-shaped 304 stainless steel



### 3. Results and Discussion

#### 3.1 Iron aluminide coatings

##### 3.1.1 Iron aluminide coatings with iron aluminide powder as the feed material

In Series A tests, iron aluminide powder was used as the feed material. In the process, the plasma voltage was fixed at 40 V, while the plasma current was varied from 20 to 40 to 60 amperes. First of all, the apparent quality of the coatings as a function of the plasma current was examined. Optical micrographs, as shown in Figure 7a, indicate that the coatings obtained with the low plasma currents (20 or 40 A), have considerable amounts of porosity at the coating/substrate interfaces, which would result in poor bonding between the coating and the substrate. In fact, the bonding of these specimens was so poor that the coatings delaminated from the substrates during either cooling or sample sectioning afterwards. The bonding is considerably improved, however, when the plasma current was increased to 60 A. Figure 7b shows that the coatings with excellent coating-substrate bonding were obtained with 60A plasma current.

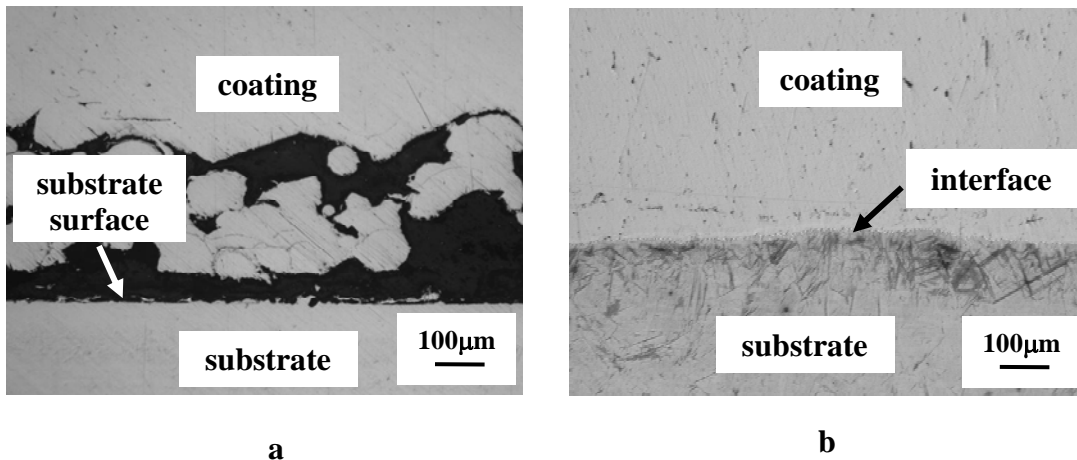


Fig.7 Cross-sectional images of coatings obtained with pre-alloyed iron aluminide powder as the feed material at different heat input powers: a. plasma current 40A; b. plasma current 60A.

To examine the possible reactions of the powder with the substrate, the profiles of

aluminum and iron contents across the coating layer obtained with the plasma current of 60 A were determined, as shown in Figure 8.

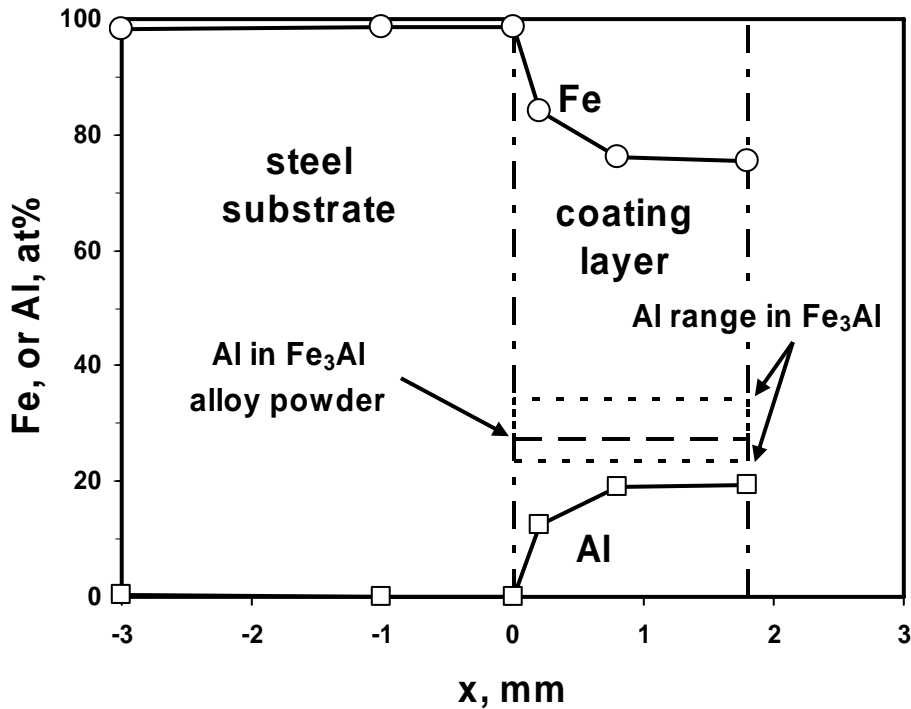


Fig.8 Variation of coating composition with pre-alloyed iron aluminide powder as the feed material.

The aluminum content in the original iron aluminide powder used in the test was Al = 27.27 at%, while the maximum Al content in the resultant coating was 19.5 at% which is only 71.4% of original Al content in iron aluminide powder. This indicates that there was significant dilution of the  $\text{Fe}_3\text{Al}$  powder by the steel substrate. It can be further reasoned that the higher plasma current, i.e. the higher plasma heat input, increases the depth of melting of the substrate surface which in turn results in more dilution. In order to obtain phase pure  $\text{Fe}_3\text{Al}$  coating, the plasma current should be kept at a minimum. On the other hand, however, as shown earlier, when the plasma current is lowered, the porosity in the coating increases and the bonding

between the coating and the substrate deteriorates. To overcome these contradicting factors, one solution to the problem is to use a relatively high plasma current to ensure good bonding and low porosity, while increasing the aluminum content in the feed powder to compensate for the inevitable dilution. This can be done by the use of blend of elemental aluminum and iron powders.

### 3.1.2 Iron aluminide coatings with blend of elemental iron and aluminum powders as the feed material

In Series B tests, a blend of elemental iron powder and aluminum powder was used as the feed material. The nominal composition of the blended powder was equivalent to  $\text{Fe}_3\text{Al}$ , i.e.,  $\text{Al}/(\text{Fe}+\text{Al}) = 25 \text{ at\%}$ . Two types of gases – pure argon or argon plus 5vol% hydrogen - were used in this series of experiments. When pure argon was used, the results showed that dense coatings could not be produced, which was attributed to the significant oxidation of the aluminum and/or iron powders. It is likely that oxidation occurred before the two powders had any chance to melt and react with each other. The oxidized surfaces of aluminum and/or iron powders would prevent not only the wetting and reaction between the two powders but also the adhesion of the coating to the steel substrate. When a mixed gas of argon plus 5 vol%  $\text{H}_2$  was used, however, satisfactory coatings with sound appearance and bonding and minimum porosity were obtained. It appears that a small amount of hydrogen added in the argon can prevent the oxidation. Figure 9 shows the profile of aluminum content across the coating layer, obtained using a plasma voltage of 40 V and a plasma current of 60 A. Although the original aluminum content in the feed powder was 25 at%, the maximum Al content in the resultant coating was only 11.6 at%. This result shows that when a blend of elemental Al and Fe powders is used,

dilution of aluminum content in the coating layer is even more severe than when pre-alloyed  $\text{Fe}_3\text{Al}$  powder is used as the feed material. The next series of experiments were therefore designed to use pure aluminum powder as the feed material.

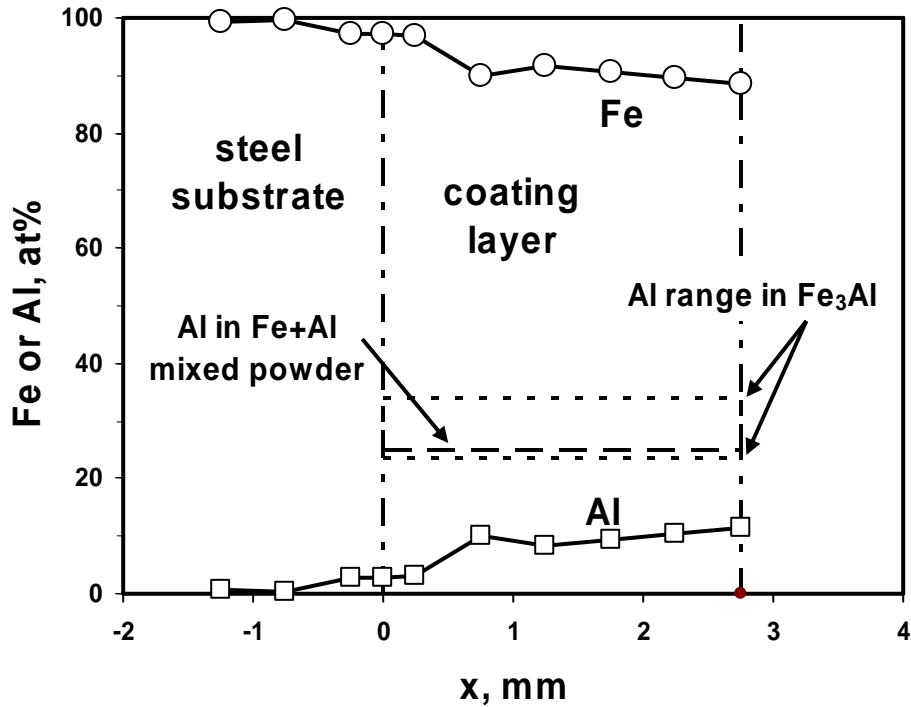


Fig.9 Variation of coating composition with a blend of Fe powder and Al powder as the feed material.

### 3.1.3 Iron aluminide coatings with aluminum powder as the feed material

In Series C tests, pure aluminum powder was used as the feed material. The argon-5vol% hydrogen mixture was used as the carrier, plasma, and shielding gases. The plasma voltage was fixed at 40 V, while the plasma current was varied at 20, 30, 40, 50, 60, 70, 75 and 80 A.

When plasma currents were 50 A or higher, continuous coating layers were formed and excellent metallurgical bonding was achieved between the coating and the substrate, as shown in Figure 10a. When the plasma currents were lower than 40 A, there were significant amounts of

pores in the coating, as shown in Figure 10b, indicating insufficient melting of Al powder and steel substrate surface and/or insufficient reaction between Al and Fe due to low heat input.

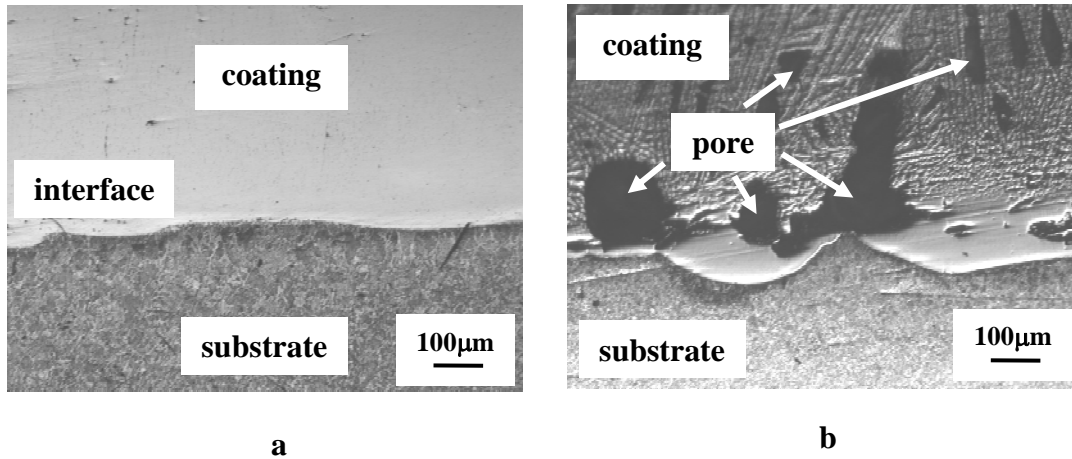


Fig.10 Cross-section of coating-substrate interface formed with Al powder as the feed material at different heat input powers: a. plasma current 50A; b. plasma current 40A.

Compositional analysis across the coating layers obtained using a 50 A or higher current, as shown in Figure 11, suggests that the composition in the obtained coating is uniform. Figure 12 shows a plot of Al content vs. the current. It shows that when the current was 60A, the composition of coating was consistent with that of the  $Fe_3Al$  phase. The phase identification was further confirmed by X-ray diffraction analysis of the 60A specimen. Figure 13 shows that the coating consists of the  $Fe_3Al$  phase with no noticeable presence of other phases.

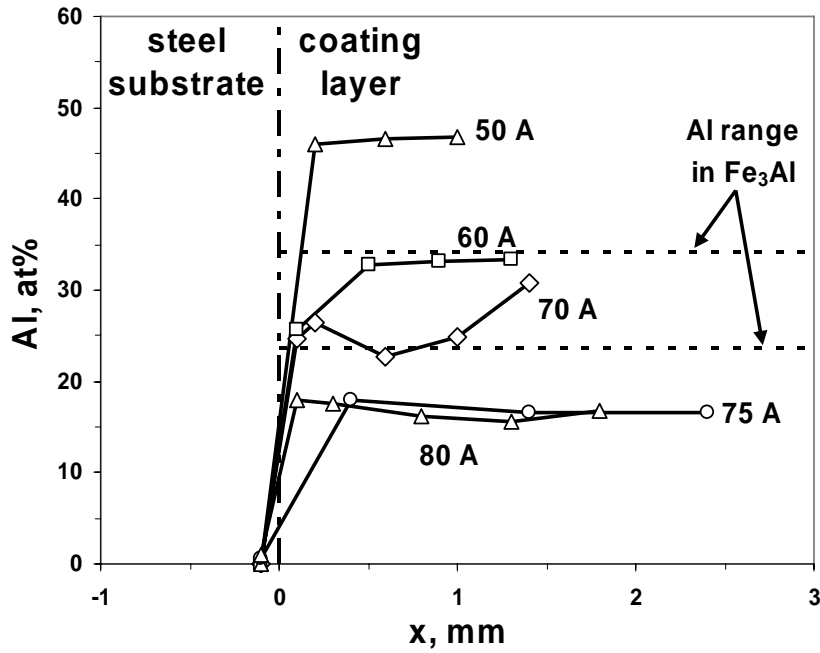


Fig. 11 Al contents in coatings (with Al powder as the feed material) obtained at different plasma currents. Note: The value beside each plot is the plasma current, while the plasma arc voltage was kept at around 40 V for all tests.

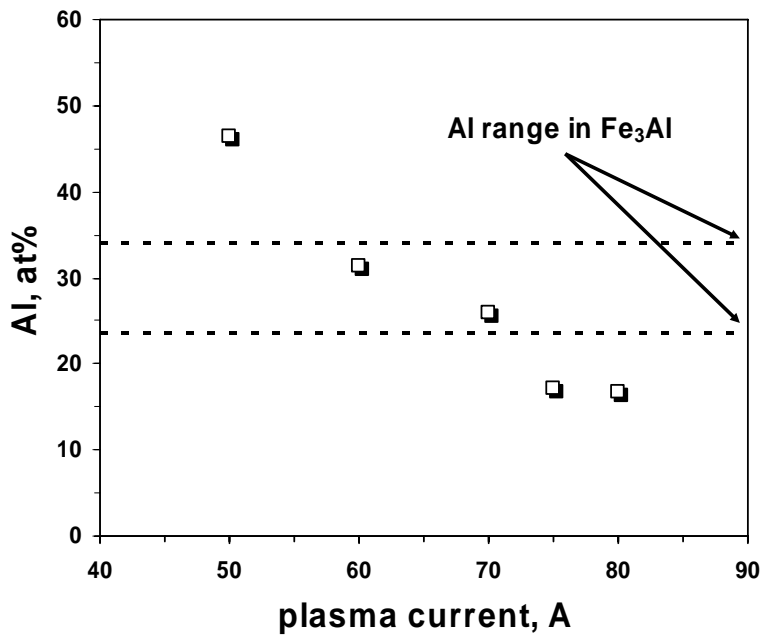


Fig.12 Al contents in coatings with Al powder as the feed material vs. the employed plasma currents

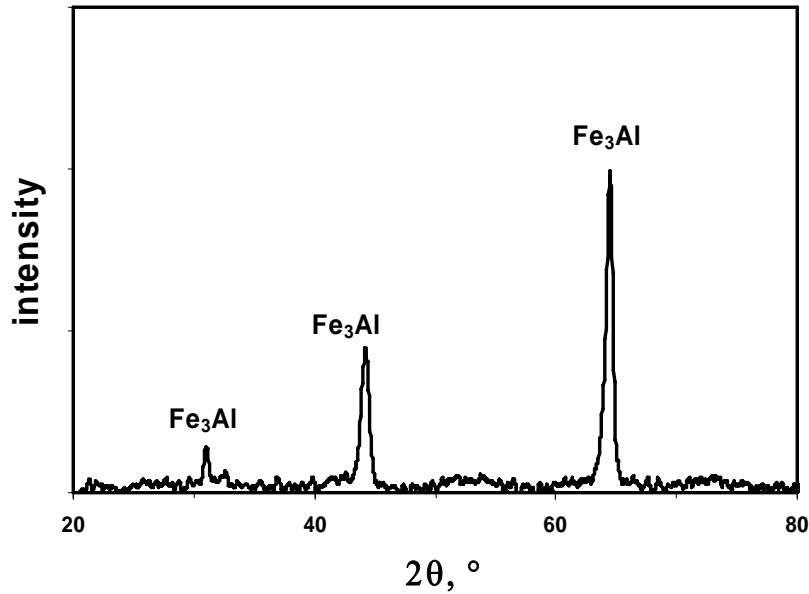


Fig.13 X-ray diffraction pattern of the coating obtained at plasma current of 60 A, with Al powder as the feed material. With Cu K $\alpha$  radiation.

When plasma currents of higher than 70 A were used, the Al contents in the coatings were lower than that of Fe<sub>3</sub>Al, which is attributed to the excessive dilution due to excessive melting of the substrate surface. The results also show that when the plasma current is lower than 60 A, the supply of iron from the steel substrate was insufficient for the reaction with Al to form an Fe<sub>3</sub>Al coating. Overall, the results suggest that 60 to 70 A is optimum for obtaining iron aluminide coatings when using pure aluminum powder as the feed material.

Bonding strength between the obtained coatings and the substrates were also evaluated by the three-point bending test. The tested sample was found to bend in the mode of good bonding, i.e., without delamination of the coating from the substrate, as shown in Figure 14, indicating excellent bonding between the coating from the substrate.

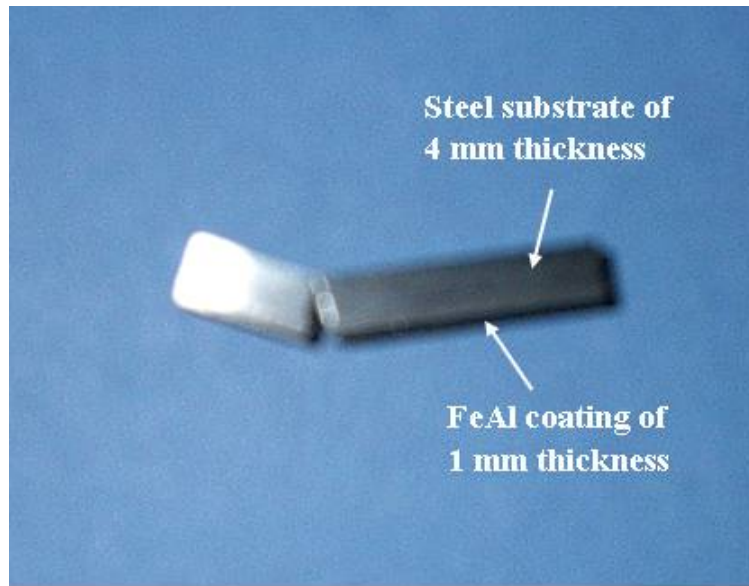


Fig. 14 Fe<sub>3</sub>Al coated on steel substrate, after three-point bending test

It is worth pointing out that the optimum plasma current will depend on the ratio the feeding rate of aluminum powder and the supply rate of the melted iron from the substrate surface which is a function of the net heat flux towards the substrate surface. The net heat flux is the difference between the heat influx from the plasma torch and heat dissipation away from the substrate surface. It is anticipated that the optimum plasma current will increase with enhanced substrate cooling by, e.g., using forced air or water cooling underneath the substrate.

#### 3.1.4 Corrosion resistance of the coatings

For the steam-side corrosion performance, as shown in Figure 5, the cross-sectional images of the samples of Fe<sub>3</sub>Al coated on steel substrate indicated that there was merely very slight corrosion on the surface of Fe<sub>3</sub>Al coatings which can be verified from the fact that the surface of Fe<sub>3</sub>Al coatings became brownish from the originally white color, while the steel substrates suffered a severe corrosion which can be identified from the thick black layer of oxide



developed on the surface of steel substrate, indicating that the corrosion resistance of  $\text{Fe}_3\text{Al}$  coatings are much more superior than common steel. The appearance of stainless steel (304) samples showed that there formed black oxide films on the surface, and some of the oxide films were found to be delaminated or even peeled off from the samples. In comparison, the cross-sectional images near  $\text{Fe}_3\text{Al}$  coating surface and near stainless steel surface are given in Figure 6 and figure 7, respectively. It is clear that the surface of  $\text{Fe}_3\text{Al}$  coating is quite clean without any obvious oxide film, while the non-continuous oxide film can be clearly seen on the surface of stainless steel. Therefore, it can be concluded that the corrosion resistance of  $\text{Fe}_3\text{Al}$  coatings is much superior to 304 stainless steel.

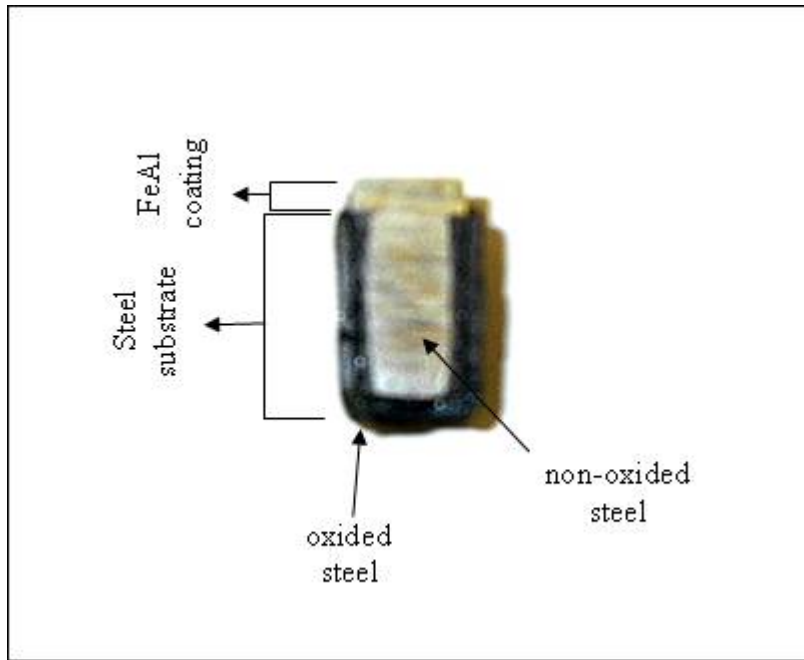


Fig. 15. Cross-sectional image of  $\text{Fe}_3\text{Al}$  coated on steel substrate, after corroded in the atmosphere of air + 10vol% water vapor at  $800^\circ\text{C}$  for 4x20 hours

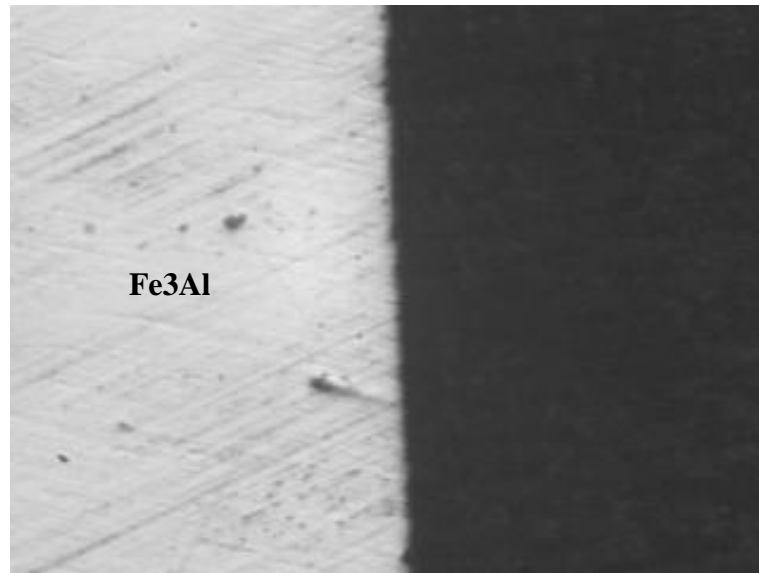


Fig. 16. Cross-sectional image of the surface of Fe<sub>3</sub>Al coating, after corrosion test

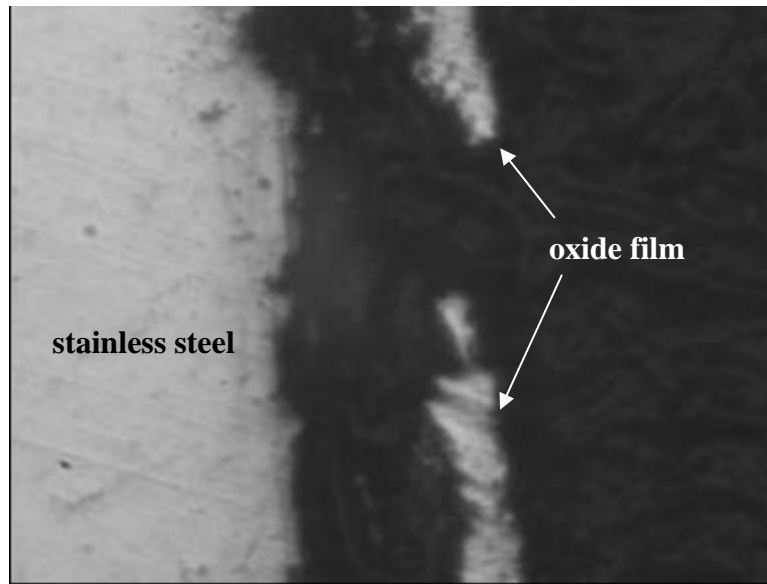


Fig. 17. Cross-sectional image of the surface of 304 stainless steel, after corrosion test

For the fire-side corrosion performance, observation of the  $\text{Fe}_3\text{Al}$  and 304 stainless steel samples after the fire-side corrosion tests showed that no observable corrosion layer developed on the surface of  $\text{Fe}_3\text{Al}$  at  $800^\circ\text{C}$  for up to 400 hours, while significant corrosion layer developed on and much of the corrosion layer peeled off from the surface of 304 stainless steel under the same condition, indicating that the corrosion resistance of  $\text{Fe}_3\text{Al}$  coating was much higher than that of 304 stainless steel.

### 3.1.5 Discussion

Based on the aforementioned experimental results, the plasma current must be sufficiently high to cause adequate melting of a substrate surface layer in order to obtain dense coatings that are metallurgically bonded to the substrates. The substrate melting, however, dilutes the coating composition. Consequently, when either pre-alloyed iron aluminide powder or

a blend of elemental Al and Fe powders was used as the feed material, the aluminum content in the coating was lower than that required for forming the  $\text{Fe}_3\text{Al}$  intermetallic compound. When pure aluminum powder was used as the feed material, the iron supply rate from the melted substrate surface could be manipulated by controlling the heat influx from the plasma torch so that the iron supply rate matched the aluminum powder feed rate to form coatings with compositions equivalent to iron aluminide. In this way, the iron aluminide coatings could be produced by the in-situ reaction between the fed aluminum powder and the iron present in the substrate.

In a typical in-situ reaction coating process, the substrate supplies part or all of one or more constituents for a binary or multi-component coating. The substrate surface reacts with the feed material to form a coating of a desired composition. The fed powder, the substrate surface, and the coating layer need to be in liquid state for a sufficient period of time during the coating process to allow the in-situ reaction to be completed. Otherwise, unreacted powder may remain in the coating layer, resulting in a coating of low quality. Therefore, a sufficiently high heat influx towards the substrate surface is necessary for the success of an in-situ reaction coating process. In this respect, the PTA technique is uniquely suitable compared to other thermal spray techniques, because the PTA torch is designed to offer a heat flux towards the substrate high enough for the substrate surface to melt. In other thermal spray coating processes, such as arc spray [21], low pressure plasma spray [22], air plasma spray [23] and high velocity oxyfuel (HVOF) spray [24-28], the torches are designed to operate with a “cold” (in comparison to the melting point of the substrate) substrate surface and thus no surface melting can occur. It is interesting to note that the dilution from the substrate, which is inevitable in the PTA process and usually regarded as a disadvantage in comparison with other thermal spray techniques, is a pre-

requisite for an in-situ reaction coating process to be successful.

Finally, it is noted that the principles of the in-situ reaction coating process demonstrated in this research are applicable to the production of coatings based on other binary or multi-component intermetallic and alloy systems. For example,  $\text{Ni}_3\text{Al}$  coatings should be formed on Ni or Ni-based alloy substrates by using Al powder as the feed material; or FeCrAl coatings should be formed on steel substrates by using a blend of elemental powders of Al and Cr.

### **3.2 Nickel aluminide coatings**

A series of coating tests were conducted to prepare nickel aluminide coatings on Ni-based alloy (more specifically Inconel 600 with the composition at% of Ni 73, Cr 17.3 and Fe 9.7) by an in-situ reaction coating process. The nickel aluminide coating was formed by an in-situ reaction between the aluminum powder fed through a plasma transferred arc (PTA) torch and the Ni-based alloy substrate. Subjected to the high temperature within an argon plasma zone, aluminum powder and the surface of alloy substrate melt and react to form the nickel aluminide coating.

The argon-5vol% hydrogen mixture was used as the carrier, plasma, and shielding gases. The plasma voltage was fixed at 40 V, while the plasma current was varied at 30, 40, 45, 50, 65 and 75 A.

When plasma currents were 40 A or lower, it was hard to obtain continuous coating layers, due to in-sufficient heat input towards the coating layer as well as the substrate surface. While plasma currents were 45 A or higher, continuous coating layers were formed, and as shown in Figure 18 the coatings were found to be porosity-free and metallurgically bonded to the substrate. It was found that the optimum plasma current was 45-65 A, because discontinuous

coatings formed when the plasma current was lower than 45A, while aluminum content in coatings was quite low when the plasma current was higher than 65A. Compositional profiles as shown in Figure 19 across the coating layer obtained in proper plasma current, e.g., 65A, suggested that the composition in the coating was quite uniform.

The average composition of the obtained coatings at the plasma current of 65 A is Al 10.08, Ni 68.41, Cr 12.93, Fe 8.00 and Mn 0.58, wt%. Since the phase diagram of Al-Ni-Cr-Fe-Mn system is not available, the above coating composition was converted to a pseudo-ternary system of Al-Ni-Cr consisting of Al 10, Ni 75.7 and Cr 14.3, wt%, via distributing Fe and Mn contents into Ni and Cr contents. Plotting the composition point of the coating in the available Al-Ni-Cr phase diagram as shown in Figure 20, it was found that the coating composition was located in the three-phase region consisting of  $\beta$ ,  $\delta$  and (Ni), where  $\beta$  is NiAl,  $\delta$  is Ni<sub>3</sub>Al and (Ni) is Ni solid solution, suggesting that the constituent phases in the coating should be NiAl, Ni<sub>3</sub>Al and (Ni). The above phase constituents in the obtained coatings were identified from the X-ray diffraction spectrum of the coatings as shown in Figure 21.

Plot of average Al contents in the coatings vs. the employed plasma current, Figure 22, indicated that aluminum content in the coating layer decreased with increasing plasma input power, due to the enhanced melting rate of the substrate surface and thus higher material supply rate from the melted substrate surface.

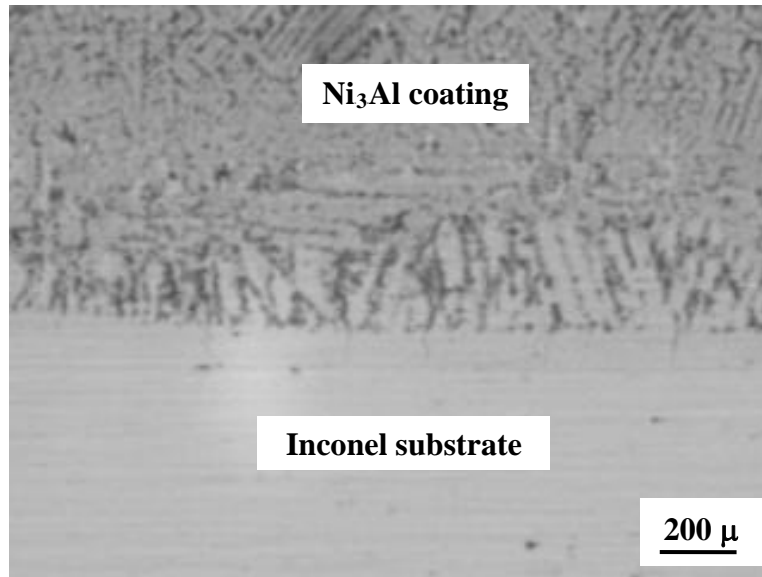


Fig. 18. Cross-sectional image at the substrate-coating interface. With pure Al as feeding materials and Inconel 600 as substrate, obtained at plasma current of 65A.

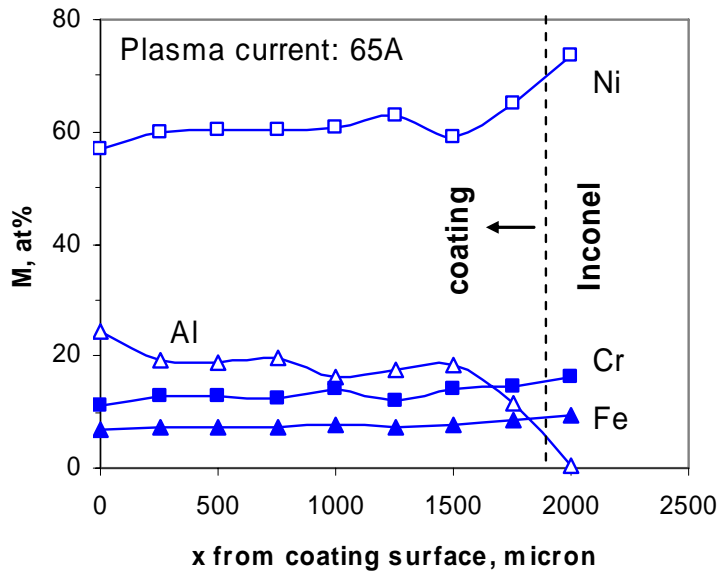


Fig. 19. Composition profiles in coating layer obtained via in-situ reaction between Al powder and Ni-based alloy substrate using PTA process, with the plasma current of 65A.

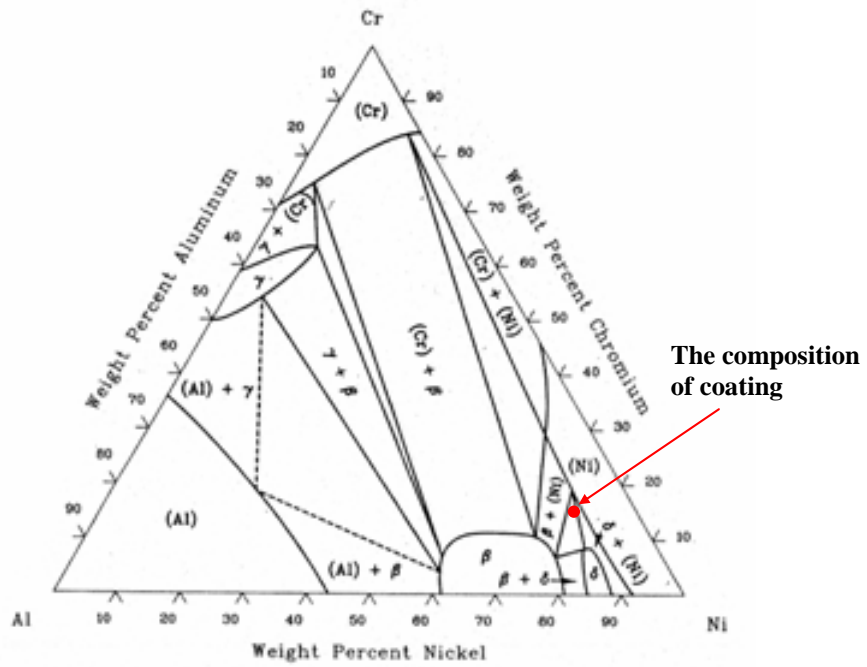


Fig. 20 Phase diagram of Al-Ni-Cr at 1323K and the composition point of the coating obtained at plasma current of 65A.

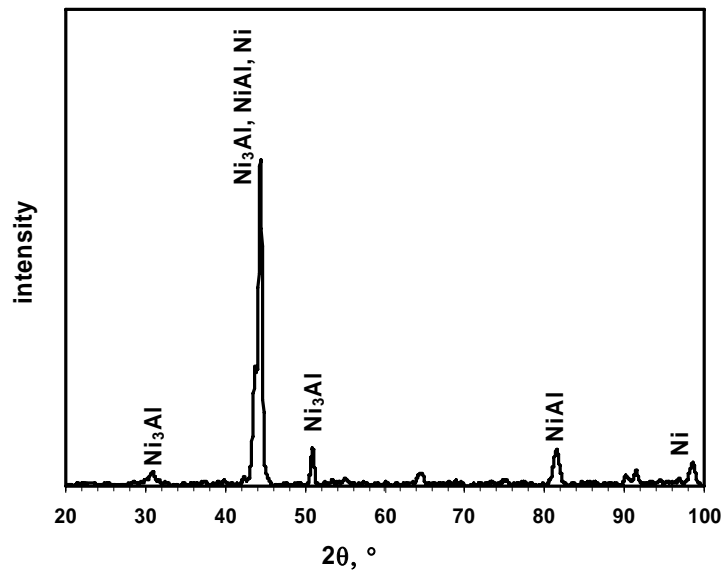


Fig. 21 X-ray diffraction spectrum of coating layer obtained at plasma current of 65A.



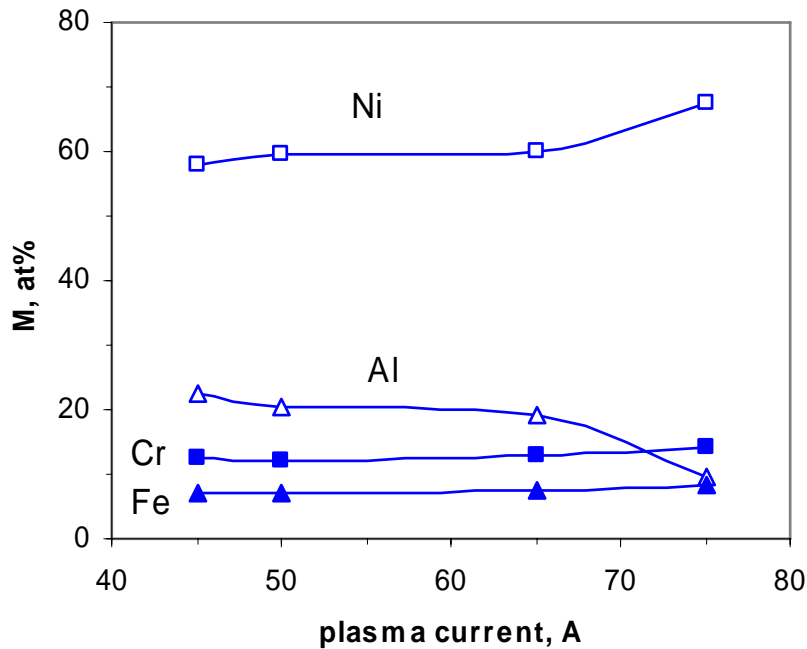


Fig. 22 Average composition of each coating layer vs the plasma current employed to obtain each coating layer.

### 3.3 Field-testing Fe<sub>3</sub>Al coating in power plant

After optimizing the coating operation parameters for achieving Fe<sub>3</sub>Al coatings on stainless steel, Fe<sub>3</sub>Al coatings have been successfully deposited on half-circle-shaped stainless steel pipes for field-test, as shown in Figure 23. The metallographic analysis indicated that the coatings were porosity-free and uniform Fe<sub>3</sub>Al that was metallurgically bonded to steel substrates.

In Sept. 20, 2007, the above two samples were mounted as shields for boiler pipes in Unit 2 Boiler, Hunter Plant, PacificCorp to start field-testing the corrosion resistance of Fe<sub>3</sub>Al coatings in realistic industry environment.

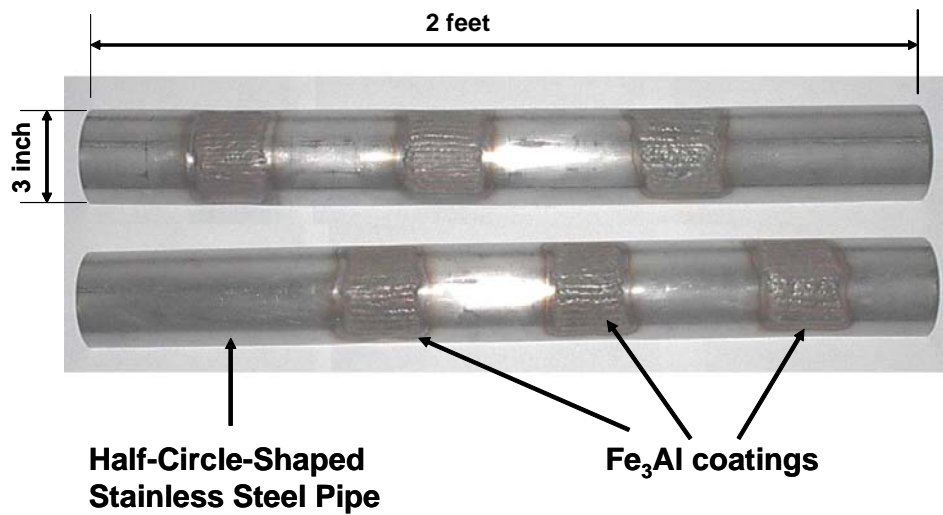


Fig. 23  $\text{Fe}_3\text{Al}$  coated stainless steel pipes which is now under field-test. Mounted in Unit 2 Boiler, Hunter Plant, PacificCorp in Sept. 20, 2007.

The shields were installed on the screen tubes directly upstream of the finishing superheater. These screen tubes are water circuits. The gas temp in this area is ~1500 deg F. The internal water temperature should correspond to saturation at essentially the drum pressure (nominally 2700 psi) or 680 degrees F. The air space between the shield and the tube and the shield is closer to the 1500 deg F gas temp.

After tested for nearly 8 months, one of the tested samples was taken out of the boiler for examination of the corrosion-resistant performance of the coating, while another sample is still in test in the boiler. The examination of the taken-out sample showed that there was no obvious corrosion on the coating, indicating excellent corrosion resistance of the  $\text{Fe}_3\text{Al}$  coatings.

#### 4. Conclusions

Based on the results presented above, the following conclusions are drawn:

1. A novel in-situ reaction process for depositing intermetallic aluminide coatings on steel or

Ni-base alloy substrates was developed. In this process, aluminum powder was fed through a plasma transferred arc (PTA) torch onto the steel substrate surface. Experimental results demonstrated that the aluminide coating was formed by an in-situ reaction between the aluminum powder and the metal substrate.

2. Coatings prepared under optimum conditions were iron aluminide or nickel aluminide that is porosity-free and metallurgically bonded to the substrate.
3. Prepared iron aluminide coatings exhibited excellent corrosion resistance in both the conditions simulating steam-side and fire-side environments in coal-fired boilers.
4. It is expected that the principle demonstrated in this process can be applied to the deposition of other intermetallic and alloy coatings.

## **Accomplishments**

### **Peer-reviewed journal articles**

Iron aluminide coating by an in-situ reaction process, P. Fan, E. Riddle, Z.Z. Fang and H.Y. Sohn, *Surface and Coating Technology*, 2008, vol.202, No.24, pp.6090-6094.

### **Conference presentations**

Iron aluminide coating produced by plasma transferred arc process, P. Fan, E. Riddle, Z.Z. Fang, H.Y. Sohn and M.D. Clark, 8<sup>th</sup> *International Conference on Trends in Welding Research*, June 2008, presented.

### **US Patent Applications**

Processes for in-situ coating of metals, Z.Z. Fang, H.Y. Sohn, P. Fan and E. Riddle, *U.S. Patent Application*, 2007, Serial No. 61/018,162.

## References

1. N. S. Stoloff, *Mater. Sci. Eng.* **A258** (1998), p.1.
2. U. Prakash, R. A. Buckley, H. Jones, and C. M. Sellars, *ISIJ International* **31** (1991), p.1113.
3. C. G. McKamey, J. H. DeVan, P. F. Tortorelli, and V. K. Sikka, *J. Mater. Res.* **6** (1991), p.1779.
4. P. F. Tortorelli and K. Natesan, *Mater. Sci. Eng.* **A258** (1998), p.115.
5. R. Viswanathan and W. T. Bakker, *J. Mater. Eng. Perf.* **10** (2001), p.81.
6. P. Tomaszewicz and G. R. Wallwork, *Oxidation of Metals* **19** (1983), p.165.
7. N. Babu, R. Balasubramaniam, and A. Ghosh, *Corros. Sci.* **43** (2001), p.2239.
8. R. Prescott and M. J. Graham, *Oxidation of Metals* **38** (1992), p.73.
9. W. D. Cho, I. Kim, and H. J. Kim, *J. Mater. Sci.* **35** (2000), p.4695.
10. K. R. Luer, J. N. DuPont, and A. R. Marder, *Corrosion* **56** (2000), p.189.
11. J. H. DeVan and P. F. Tortorelli, *Corros. Sci.* **35** (1993), p.1065.
12. P. F. Tortorelli and J. H. DeVan, *Mater. Sci. Eng.* **A153** (1992), p.573.
13. P. C. Patnaik and W. W. Smeltzer, *J. Electrochemical Soc.* **132** (1985), p.1226.
14. B. A. Pint, Y. Zhang, P. F. Tortorelli, J. A. Haynes, and I. G. Wright, *Materials at High Temperatures*, **18** (2001), p.185.
15. C. Christoglou, N. Voudouris, G.N. Angelopoulos, *Surf. Coat. Tech.* **155** (2002), p.51.
16. L. Sanchez, F.J. Bolivar, M.P. Hierro, J.A. Trilleros, and F.J. Perez, *Surf. Coat. Tech.* **201** (2007), p.7626.
17. R. Sivakumar, E.J. Rao, *Oxidation of Metals* **17** (1982), p.391.
18. R. Mevrel, C. Duret, R. Pichoir, *Mater. Sci. Tech.* **2** (1986), p.201.

19. L. Levin, A. Ginzburg, L. Klinger, T. Werber, A. Katsman, P. Schaaf, *Surf. Coat. Tech.* **106** (1998), p.209.
20. Z.D. Xiang and P.K. Datta, *Acta Mater.* **54** (2006), p.4453.
21. B. H. Tian, B. S. Xu, S. N. Ma, W. Zhang, J. Z. Hu, and X. B. Liang, in *Mechanics and Materials Engineering for Science and Experiments*, Y.C. Zhou, Y.X. Gu and Z. Li, ed. Changsha/Zhangjiajie, China (2001), p.417.
22. N. Masahashi, S. Watanabe, and S. Hanada, *ISIJ International*, **41** (2001), p.1010.
23. R.N. Wright, J.R. Fincke, W.D. Swank, D.C. Haggard, and C.R. Clark: in *Elevated Temperature Coatings: Science and Technology I*, N.B. Dahotre, J.M. Hampikian, and J.J. Stiglich, ed., TMS, Warrendale, PA, (1995), p.157.
24. J.R. Blackford, R.A. Buckley, H. Jones, C.M. Sellars, D.G. McCartney and A.J. Horlock, *J. Mater. Sci.* **33** (1998), p.4417.
25. T. Grosdidier, H.L. Liao, and A. Tidu: in *Thermal Spray: Surface Engineering Via Applied Research*, C.C. Berndt, ed., ASM International, Materials Park, OH, (2000), p.1341.
26. T. C. Totemeier, R. N. Wright, and W. D. Swank, *J. Thermal Spray Tech.*, **11** (2002), p.400.
27. B. Szczucka-Lasota, B. Formanek and A. Hernas, *J. Materials Processing Technology*, **164**(2005), p.930.
28. J.M. Guilemany, N. Cinca, S. Dosta and C.R.C. Lima, *Intermetallics*, **15**(2007), p.1384.
29. T. Owa, T. Shinoda, and Y. Katoh, *J. Japan Inst. Metals*, **65** (2001), p.509.
30. T. Owa and T Shinoda, *J. Jap. Welding Soc.*, **22** (2004), p.494.
31. R. Hultgren, P. Desai, D.T. Hawkins, M. Gleiser and K.K. Kelley, *Selected values of the thermodynamic properties of binary alloys*, ASM, Metals Park, Ohio (1973), p.161.